

# The 7th International Symposium on Linear Drives for Industry Applications

September 20~23, 2009  
Hyatt Regency Incheon, Korea

- Welcome Message
- September 21, 2009 (Monday)
- September 22, 2009 (Tuesday)
- Author Index
- Search
- Help
- Exit



PS1.9	A Linear Motor Designed with Grain-oriented Silicon Steel Sheets Takashi Todaka (Oita Univ., Japan), Motomichi Ohto (Yasukawa Electric Co., Ltd., Japan), and Masato Enokizono (Oita Univ., Japan) .....	28
PS1.10	Force Calculation of Linear Switched Reluctance Machine According to Design Parameters Ji-Hoon Park, Seok-Myeong Jang, Dae-Joon You, So-Young Sung (Chungnam Natl Univ., Korea), and Han-Wook Cho (KIMM, Korea) .....	30
PS1.11	Analysis on the Static Characteristics of Infinitely Operated Linear Synchronous Machine with Halbach Array Permanent Magnet Kyoung-jin Ko, Seok-Myeong Jang, Ji-Hoon Park, Cheol-Soo Coo, Jang-Young Choi (Chungnam Natl Univ., Korea), and Sung-Ho Lee (Korea Inst. Industrial Tech., Korea) .....	32
PS1.12	Application of Flux Concentrated Permanent Magnet Arrangement with Halbach Array for 2-pole PMLSM Shunji Tahara, Yuta Ishida, and Kokichi Ogawa (Oita Univ., Japan) .....	34
PS1.13	Flux Distribution and Thrust of PMLSM with Concentrated Magnet Arrangement Yuta Ishida, Shunji Tahara, and Kokichi Ogawa (Oita Univ., Japan) .....	36
PS1.14	Electromagnetic Thrust Analysis and Dynamic Simulation for Evaluating Jerk Characteristics of Linear Induction Motor Seok-Myeong Jang, Yu-Seop Park, Ji-Hoon Park, Jin-Soon Kim (Chungnam Natl Univ., Korea), Dae-Joon You (Cheongyang Provincial College, Korea), and So-Young Sung (Chungnam Natl Univ., Korea) .....	38
PS1.15	Bidirectional Motion Control of Double-sided LSM with Slotless Iron-cored Stator and PM Mover Using Design Parameters and Discrete System Modeling Seok-Myeong Jang, Ji-Hwan Choi, Ji-Hoon Park (Chungnam Natl Univ., Korea), Dae-Joon You (Cheongyang Provincial College, Korea), Il-Jung Kim (Hoseo Univ., Korea), and Kyoung-Bok Lee (Daejeon Express Transit Corp., Korea) .....	40
PS1.16	Estimation Performance According to Goodness Factor of Tubular Linear Induction Motor Jeong-Jong Lee, Byeoung-Hwa Lee, Soon-O Kwon, Sung-Il Kim, and Jung-Pyo Hong (Hanyang Univ., Korea) .....	42
PS1.17	A Study on Auxiliary Core Design of PMLSM to Reduce Detent Force by End Effect Jee-Hyun Kim (Changwon Natl Univ., Korea), Ho-Jin Ahn (Cyeongnam Technopark, Korea), Ki-Bong Jang, and Cyu-Tak Kim (Changwon Natl Univ., Korea) .....	44

# Estimation performance according to Goodness factor of Tubular Linear Induction Motor

Jeong-Jong Lee<sup>†</sup>, Byeoung-Hwa Lee<sup>†</sup>, Soon-O Kwon<sup>†</sup>, Sung-Il Kim<sup>†</sup>,  
and Jung-Pyo Hong<sup>†</sup>

<sup>†</sup> Department of Automotive Engineering, Hanyang University, Korea  
Tel: +82-02-2220-4466 – Fax: +82-02-2220-4465 – e-mail: [motor@hanyang.ac.kr](mailto:motor@hanyang.ac.kr), [hongjp@hanyang.ac.kr](mailto:hongjp@hanyang.ac.kr)

Topics: 11

## 1. Introduction

Linear motors make good use of several applications as pumps and linear actuator. Generally rotary type electric machines are widely used; however, applying rotary machines to linear system have limitations. Also, when rotary machines are used for linear moving systems, additional mechanical losses due to gears, ball screw, and belts are inevitable, and the system become complex and inefficient. Various designs of linear motors are studied to overcome such limitations of rotary machines. One of them is the short primary member tubular linear induction motor (TLIM). Figure 1 shows the structure of TLIM. The primary core in TLIM is made of several disc or transversal lamination of ferromagnetic material. The main advantages of the TLIM are that it is rugged and easy to build. Because of TLIM is used at a very low speed, the dynamic end effects are negligible and the static end effect can be minimized by good design [1], [2]. However, due to the more complex geometry and difficult physical phenomena in TLIM compared to single-sided linear induction motor (SLIM), special attention must be paid particularly core saturation, eddy current induced in the core and skin effect analysis in the secondary conductor sheet.

The main object of this paper is concerned with the characteristic analysis to thickness of secondary conductor in TLIM which is capable of application to the elevator system. Characteristic equations of TLIM are obtained from voltage equation. Using by finite element method (FEM), parameters of voltage equation are calculated. To consider secondary conductor effect FEM is performed at time-harmonic field. And secondary resistance loss is calculated by eddy current using FEM.

Consequently, the thrust force of TLIM according to goodness factor of secondary conductor thickness is compared. And then, this paper presents how to decide secondary conductor resistance at motor design. The end results are presented in a useful form.

## 2. Methodology

### 2.1. Equivalent circuit

Figure 2 show the equivalent circuit of TLIM each phase in steady-state mode. Equation (1) and (2) are voltage equation of TLIM[3].

$$U_s = I_s (R_1 + j\omega_1 L_1) + (I_s + I_t)(j\omega_1 L_m) \quad (1)$$

$$0 = I_t \left[ \left( \frac{R_2}{s} \right) + j\omega_1 L_2 \right] + (I_s + I_t)(j\omega_1 L_m) \quad (2)$$

Where,  $U_s$  is effective value of secondary part voltage per phase,  $\omega_1$  is angular frequency of primary part,  $I_s$  and  $I_t$  are effective value of input current in primary and secondary part,  $R_1$  and  $R_2$  are resistance of primary and secondary respectively,  $L_m$  is mutual inductance and  $L_2$  is leakage inductance of secondary part.

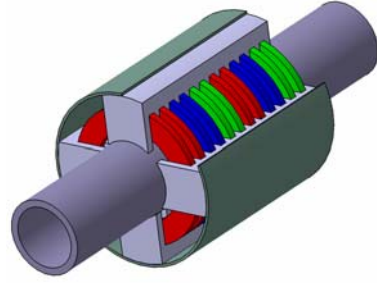


Figure 1: Structure of Tubular Linear Induction Motor

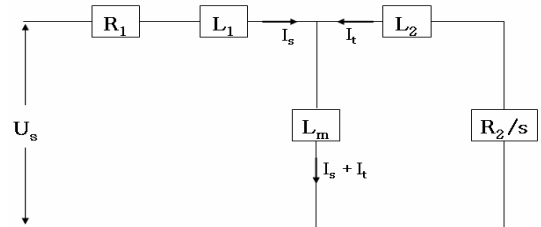


Figure 2: Equivalent circuit of TLIM per phase

### 2.2. Analysis model

Figure 3 shows the cross-section view of TLIM. Primary part consists of iron core and armature coil, and secondary parts consist of aluminium tube (the secondary conductor sheet) and an iron rod for a magnetic return yoke. Table 1 shows the specifications of analysis model of TLIM.

### 2.3. Parameter Calculation

The main parameters can be separated four parameters in TLIM. Each parameter is shown in Figure 2.  $R_1$  can be calculated linear parameter as  $R = l/\sigma S$ .  $L_1$  and  $L_m$  can be calculate by FEA(Finite Element Analysis). This model is solved the time-harmonic field analysis with real and imaginary terms. When the secondary circuit is open(slip=0), the leakage inductance can calculate by (3)

$$L_1 = \frac{\lambda_{leak}}{I_s}, \quad L_m = \frac{\lambda_{1T} - \lambda_{leak}}{I_s} \quad (3)$$

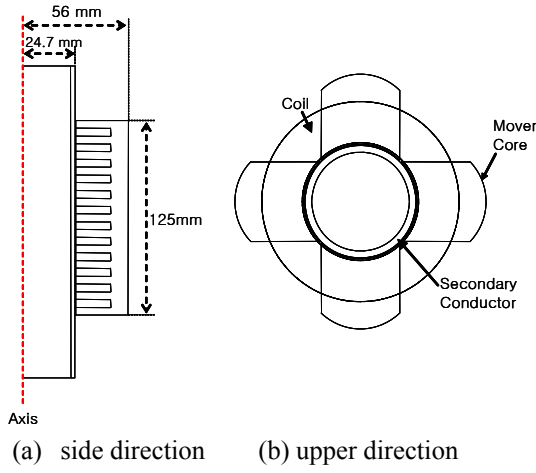


Figure 3: Structure & Cross-section view of TLIM

Table 1 : Specifications of TLIM.

Items	Specifications	Value	Unit
Normal	Voltage	110	Vrms
	Rating Current	10	Arms
	Frequency	60	Hz
	Length	125	mm
	Diameter	110	mm
stationary part	Pole/slot number	4/12	
	Series Turn number/ Phase number	400	
mover	Material	Aluminum	
	Conductor Depth	3	mm
Air gap length		0.5	mm

#### 2.4. Characteristic Analysis and Goodness factor

Characteristic equations are obtained from equivalent circuit. First, thrust force per phase is calculated using Lorentz's law. Thrust force ( $F_z$ ) is expressed

$$F_z = 3p \frac{\omega_1 I_s^2 M_{ts}^2 (\omega_1 s) T_t}{v_0 L_{tt} [1 + (\omega_1 s) T_t]} \quad (4)$$

Where,  $v_0$  is synchronous speed,  $M_{ts}$  is mutual inductance of secondary part,  $L_{tt}$  is self inductance of secondary part,  $s$  is slip and  $T_t$  is electric time constant.

And input current in equivalent circuit is calculated by input voltage.

$$I_s = U_s \frac{(R_2/s) + j\omega_1 (L_2 + L_m)}{[R_1 + j\omega_1 (L_1 + L_m)][R_2/2 + j\omega_1 (L_2 + L_m)] + (\omega_1 L_m)^2} \quad (5)$$

Also mechanical power output can be expressed by equation (5). Thrust force ( $F_z$ ) per phase times velocity ( $v_0$ ) is equal to mechanical output ( $p$ ).

$$P = F_z v = F_z (1-s) v_0 \quad (6)$$

Lastly, power factor ( $\cos\phi$ ) and efficiency ( $\eta_1$ ) are

defined by mechanical power output per unit air-gap volt amps for TLIM is given by equation (7) and (8).

$$\cos\phi = \frac{F_z 2\tau f_1 + 3R_1 I_s^2}{3pU_s I_s} \quad (7)$$

$$\eta_1 = \frac{F_z 2\tau f_1 (1-s)}{F_z 2\tau f_1 + 3R_1 I_s^2} \quad (8)$$

where,  $\tau$  is pole pitch and  $f_1$  is frequency of primary part.

The goodness factor  $G$  is given by equation (9)

$$G = \frac{X_m}{r_2} \quad (9)$$

where,  $X_m$  is magnetizing reactance and  $r_2$  is secondary resistance.

### 3. Result and Discussion

#### 3.1. Equivalent parameter of analysis model

Table 2 shows the equivalent parameter of TLIM according to thickness of secondary conductors. In table 2, the value of  $G$  means the goodness factor. This factor is smaller as thickness of conductor is larger.

Table 2 : Equivalent parameter according to secondary conductor thickness.

Items	Unit	Conductor thickness (mm)		
		2	3	4
$R_1$	$\Omega$	0.3821	←	←
$L_1$	mH	13.4	←	←
$R_2$	$\Omega$	2.04	1.36	1.02
$L_m$	mH	8.81	←	←
$G @ 60\text{Hz}$		1.63	1.73	3.25

#### 3.2. Torque and Current Characteristic

Since the TLIM stator has 12 slots, a 4-pole TLIM requires on slot per pole per phase. This leads to a pole pitch of 60mm. As a result the synchronous velocity of the TLIM at 60Hz is 3.6 m/s. Figure 4 shows the phase current according to secondary conductor thickness and velocity. Since the secondary resistance is reduced with thickness, the phase current reduced. Figure 5 shows the thrust force according to mover velocity

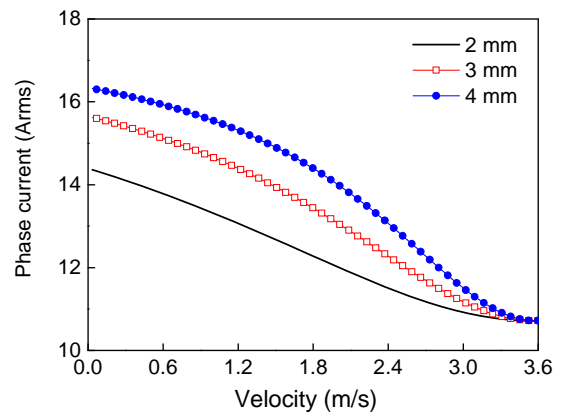


Figure 4: Phase current according to velocity

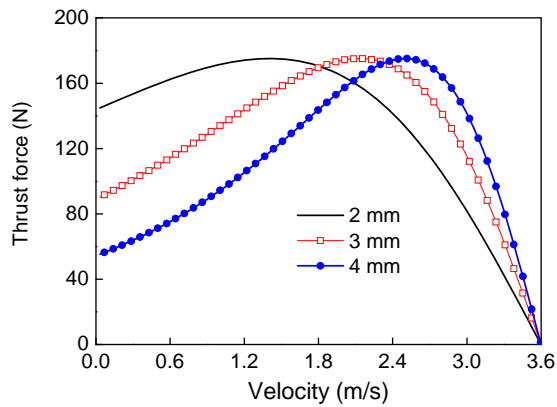


Figure 5: Thrust force according to velocity

Figure 6 shows the thrust force according to input frequency. When the frequency is reduced, the  $X_m$  is reduced proportion to frequency. Therefore the goodness factor is reducing to 1.

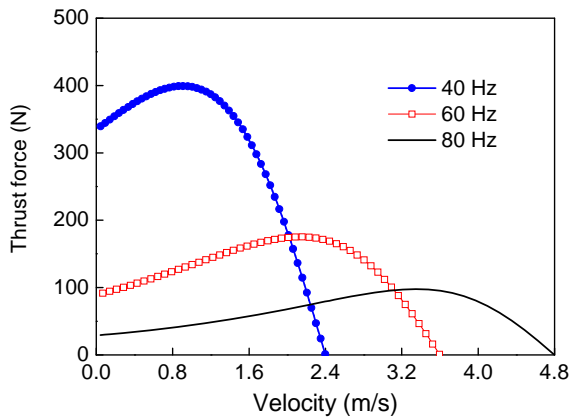


Figure 6: Operating region vs. input frequency

### 3.3. FEA Result and Conductor loss

Fig. 7 shows the equi-potential distribution. 4poles are formed by winding distributions. Fig. 7(a) is real parts of time harmonic files analysis, and 7(b) is imaginary parts.

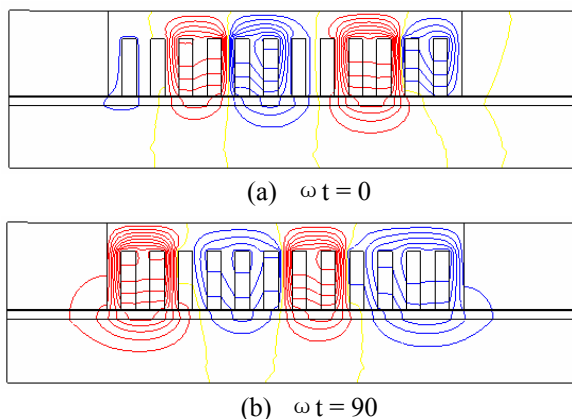


Figure 7: Equi-potential line of TLIM

Figure 8 shows the secondary part current distribution. In this paper, conductor thickness is changed to 4mm from

2mm. The total conductor loss is shown in figure 9 according to the thickness. Eddy current loss is reduced according to increased conductor thickness.

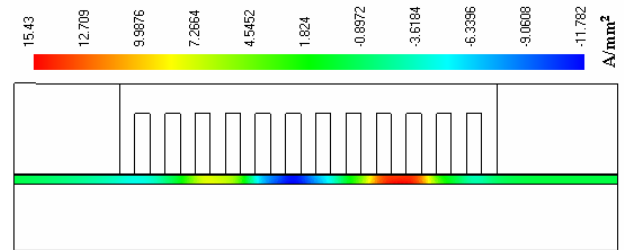


Figure 8: Current density of secondary conductor

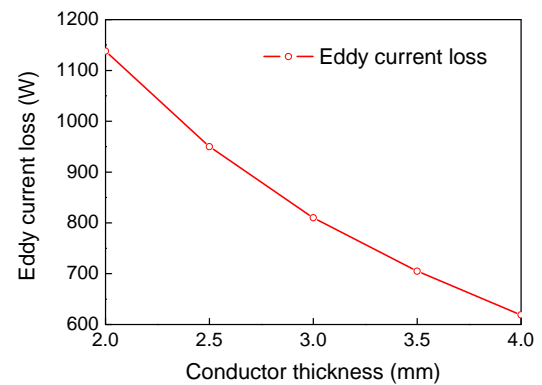


Figure 9: Eddy current loss of TLIM according to conductor thickness

## 4. Conclusion

This paper presents characteristic analysis to thickness of secondary conductor in TLIM which is capable of application to the elevator system. The modeling of the TLIM, with axis-symmetry, is used by the FEM. The eddy current loss of TLIM according to secondary conductor thickness is compared. In the paper, using by equivalent circuit analysis of TLIM according to secondary conductor thickness was conducted. And then, this paper presents how to decide secondary conductor resistance at TLIM design.

## References

- [1] Ching-Chih Tsai, Ssu-Min Hu, Chan-Kan Chang "Vertical Liner Motion System Driven by a Tubular Linear Induction Motor", IEE Proceeding, International Conference on Mechatronics, pp.162-167, July 2005.
- [2] D. Deás, P. Kuo-Peng, N. Sadowski, A. M. Oliveira, J. L. Roel, and J. P. A. Bastos, "2-D FEM Modeling of the Tubular Linear Induction Motor Taking Into Account the Movement", IEEE TRANSACTIONS ON MAGNETICS, vol. 38, No. 2, pp.1165-1168, March 2002.
- [3] Ir. D. F. de Groot, Prof. D. J. Heuvelman "Tubular Linear Induction Motor for use as a servo actuator", IEEE TRANSACTIONS ON MAGNETICS, vol. 38, No. 2, pp.1165-1168, March 2002.